



Tropical Weathering History Recorded in the Silicon Isotopes of Lateritic Weathering Profiles

Damien Guinoiseau, Zuzana Fekiacova, Thierry Allard, Jennifer Druhan, Etienne Balan, Julien Bouchez

► To cite this version:

Damien Guinoiseau, Zuzana Fekiacova, Thierry Allard, Jennifer Druhan, Etienne Balan, et al.. Tropical Weathering History Recorded in the Silicon Isotopes of Lateritic Weathering Profiles. *Geophysical Research Letters*, 2021, 48 (19), pp.e2021GL092957. 10.1029/2021GL092957 . hal-03442888

HAL Id: hal-03442888

<https://hal.science/hal-03442888>

Submitted on 23 Nov 2021

HAL is a multi-disciplinary open access archive for the deposit and dissemination of scientific research documents, whether they are published or not. The documents may come from teaching and research institutions in France or abroad, or from public or private research centers.

L'archive ouverte pluridisciplinaire **HAL**, est destinée au dépôt et à la diffusion de documents scientifiques de niveau recherche, publiés ou non, émanant des établissements d'enseignement et de recherche français ou étrangers, des laboratoires publics ou privés.



Distributed under a Creative Commons Attribution - NonCommercial - NoDerivatives 4.0 International License

Geophysical Research Letters[®]



RESEARCH LETTER

10.1029/2021GL092957

Key Points:

- Silicon isotopes in lateritic weathering profiles combined with dating tools record past weathering conditions
- Silicon isotope signatures of clays reflect the rate of water infiltration during laterite formation
- The duration and intensity of weathering episodes can be constrained using a reactive transport model

Supporting Information:

Supporting Information may be found in the online version of this article.

Correspondence to:

D. Guinoiseau,
damien.guinoiseau@universite-paris-saclay.fr

Citation:

Guinoiseau, D., Fekiacova, Z., Allard, T., Druhan, J. L., Balan, E., & Bouchez, J. (2021). Tropical weathering history recorded in the silicon isotopes of lateritic weathering profiles. *Geophysical Research Letters*, 48, e2021GL092957. <https://doi.org/10.1029/2021GL092957>





Received 1 MAR 2021

Accepted 16 SEP 2021

© 2021. The Authors.

This is an open access article under the terms of the [Creative Commons Attribution-NonCommercial-NoDerivs](https://creativecommons.org/licenses/by-nc-nd/4.0/) License, which permits use and distribution in any medium, provided the original work is properly cited, the use is non-commercial and no modifications or adaptations are made.

Tropical Weathering History Recorded in the Silicon Isotopes of Lateritic Weathering Profiles

Damien Guinoiseau^{1,2} , Zuzana Fekiacova² , Thierry Allard³ , Jennifer L. Druhan^{1,4} , Etienne Balan³ , and Julien Bouchez¹ 

¹Université de Paris, Institut de physique du globe de Paris, CNRS, Paris, France, ²Aix Marseille Univ, CNRS, IRD, INRAE, Coll France, CEREGE, Aix-en-Provence, France, ³Sorbonne Université, Université Pierre et Marie Curie, IMPMC, UMR CNRS 7590, Paris, France, ⁴Department of Geology, University of Illinois at Urbana-Champaign, Urbana, IL, USA

Abstract Under tropical climates, mineral assemblages composing lateritic weathering profiles offer precious records of past weathering conditions. Silicon (Si) isotope signatures in the clay fractions of a deep lateritic profile in central Amazonia, Brazil, in combination with previously determined kaolinite ages, suggest that the surrounding region underwent two major weathering episodes, distinct in their intensity. The first episode (ca. 35–20 Ma) of moderate intensity produced well-crystallized kaolinites from the parent sediment with limited Si isotope fractionation. A more recent (8–6 Ma) and shorter phase caused the replacement, from top to bottom of the profile, of the first kaolinite generation by a new population characterized by higher crystallographic disorder and stronger Si isotope fractionation, suggesting weathering under conditions of rapid water percolation. These inferences are supported by results from an isotope-enabled reactive transport model, and they are consistent with paleoclimatic and paleogeographic evidences recorded over the Amazon Basin.

Plain Language Summary Tropical landscapes are often covered by nutrient-depleted soils overlying lateritic weathering profiles, that result from a complex set of chemical reactions between air, water, rocks, and living organisms. Mineral phases hosted by these deep weathering profiles, such as clays, have formed from reactions between primary minerals and elements present in subsurface waters, and thus hold the potential to record local past environmental conditions. We use numerical models to show that the distribution of the various isotopes of the major clay-forming element silicon (Si) depends on the rapidity at which rainwater percolates downward through soil porosity. We demonstrate that clays present in a lateritic profile in central Amazonia formed during two distinct episodes. The first episode occurred between 35 and 20 million years ago at a time when rain in Amazonia was much less abundant than it is today. A second, shorter episode occurred between 8 and 6 million years ago under significantly wetter conditions than at present. Our study thus shows that silicon isotope analyses of lateritic profile can reveal the past evolution of climate in the tropics, which can in turn illuminate the future changes that will inevitably affect this region of our planet.

1. Introduction

Cenozoic Andean uplift has led to dramatic shifts in climate, erosion, hydrography, and biodiversity across the Amazon Basin (Albert et al., 2018; Hoorn, Roddaz, et al., 2010; Hoorn, Wesselingh, et al., 2010). In particular, the late Miocene (9–11 Ma) is a key period where the cratonic sediment source to the central Amazon Basin was supplanted by sediment supply from the Andes, due to the onset of the transcontinental Amazon River (Figueiredo et al., 2009; Hoorn et al., 2017). The impact that these changes had on chemical weathering is still a matter of debate. In this regard, old laterites can be seen as precious records of past weathering conditions. Relict populations of secondary phases such as goethite or kaolinite hosted by these deep, strongly weathered profiles hold records of the ambient conditions of their formation through their petrological, mineralogical, and geochemical characteristics (Ambrosi & Nahon, 1986; Beauvais, 1999; Girard et al., 1997, 2000; Muller & Calas, 1989; Nahon, 2003; Vasconcelos, 1999). Interpretation of lateritic weathering profiles as the result of episodic versus continuous evolution is still highly debated. Geochemical and mineralogical studies performed on Amazonian laterites hypothesized they are the result of continuous development over 15–30 Myr (Fritsch et al., 2002; Giral-Kacmarcik et al., 1998; Lucas, 1989;

Lucas et al., 1996), and of strong nutrient cycling signature due to vegetation in topsoil horizons. However, dating techniques have provided additional constraints on the formation and evolution of lateritic profiles (Allard et al., 2018; Balan et al., 2005; Mathian et al., 2020; Mathieu et al., 1995; Monteiro et al., 2018; Ruffet et al., 1996; Théveniaut & Freyssinet, 2002; Vasconcelos, 1999; Vasconcelos et al., 1994). In particular, the age distribution of secondary phases in laterites indicates that weathering processes may have occurred during discrete and relatively short events, associated with shifts in climatic or geodynamic forcing (Allard et al., 2018; Mathian et al., 2020; Retallack, 2010; Vasconcelos, 1999; Vasconcelos et al., 1994). While major processes responsible for laterite formation are known (Nahon, 2003 and references therein), limitations and uncertainties inherent to dating techniques (Allard et al., 2018; Balan et al., 2020) call for the development of independent tools to retrieve paleo-environmental conditions recorded in secondary minerals hosted by laterites. The stable isotopes of silicon (Si) are a promising tool because mass-dependent fractionation is known to occur during the formation of clays, such as kaolinite, in soils (e.g., Opfergelt et al., 2012). The main advantage of the Si isotope system lies in the fact that during chemical weathering, the characteristic signatures of both kinetic and equilibrium fractionation can be preserved in clays. The isotope expression of these two regimes of fractionation depends on the rate of clay formation; kinetically driven and equilibrium-driven fractionations are characteristic of high and low formation rates, respectively (Oelze et al., 2014, 2015). This formation rate can in turn be linked to environmental conditions, such as fluid residence time (Maher et al., 2009), at the time of mineral precipitation.

The present study focuses on a well-documented lateritic weathering profile developed over the Cretaceous-Paleogene sedimentary Alter do Chão Formation in the Amazon Basin (Lucas et al., 1996). Vertical variation in ages of kaolinite throughout the profile is interpreted to reflect the replacement of an old kaolinite generation by a more recent one. Observed vertical gradients in age and mineralogy parameters result from mixing between these two end-members (Balan et al., 2005). Here, we combine chronological constraints with new measurements of Si isotope signatures in the kaolinite clay fraction as a function of depth through the profile. We show that the Si isotope data support the previous interpretation of a bimodal distribution of kaolinite ages and mineralogy, which resulted from two weathering episodes distinct in age and intensity. Using a multicomponent numerical reactive transport model, we constrain the average fluid flow rate through the profile necessary to support the growth and Si isotope fractionation of each of the two kaolinite populations, showing that the Si isotope record is sensitive to formation conditions. In addition, we estimate the duration of the weathering episodes, which is not possible with kaolinite dating owing to poor statistics. Altogether, our study showcases the potential of Si isotopes as a tool to single out past weathering episodes in lateritic profiles, and to constrain past environmental conditions that supported these periods of formation.

2. Settings, Material, and Methods

This study focuses on a lateritic profile developed on the sedimentary Alter do Chão Formation, 50 km North of Manaus, Brazil (Figure S3). The Alter do Chão Formation consists of a ca. 300-m thick sedimentary unit deposited in the Amazon Basin from the Late Cretaceous to the Paleogene (Hoorn et al., 2010). Deposition of cratonic-derived conglomerates with sandy and clayey intercalated beds is typical of a braided fluvial system flowing toward the SW with associated alluvial fans (Horbe et al., 2006; Mendes et al., 2012). Discontinuous sedimentation is observed with edification of paleosols (Montes et al., 2002). Although the Alter do Chão sediments have most likely undergone pre-depositional weathering, the presence of iron bleaching, kaolinitized feldspar, and kaolinite booklets located in lenses in discordance with the stratification of sand beds all support the occurrence of post-depositional weathering processes (Balan et al., 2005; Fritsch et al., 2002; Irion, 1984). This is further corroborated by the 37–22 Ma ages of kaolinite in the Alter do Chão sediments (Balan et al., 2005).

Extensive pedological, geochemical, and chronostratigraphic descriptions of the studied lateritic weathering profile are available in previous studies (e.g., Balan et al., 2005; Lucas et al., 1996). Briefly, the 20-m profile considered in the present study, which corresponds to "site III" in Balan et al. (2005), comprises the weathered Alter do Chão sediment at depth and defined as a saprolite, a mottled zone and a nodular horizon topped by a loose soil called latosol (Figure 1a). Chemical composition and Si isotope analyses were performed on purified clay-sized fractions (<5 μm), checked to be free of quartz contribution, and

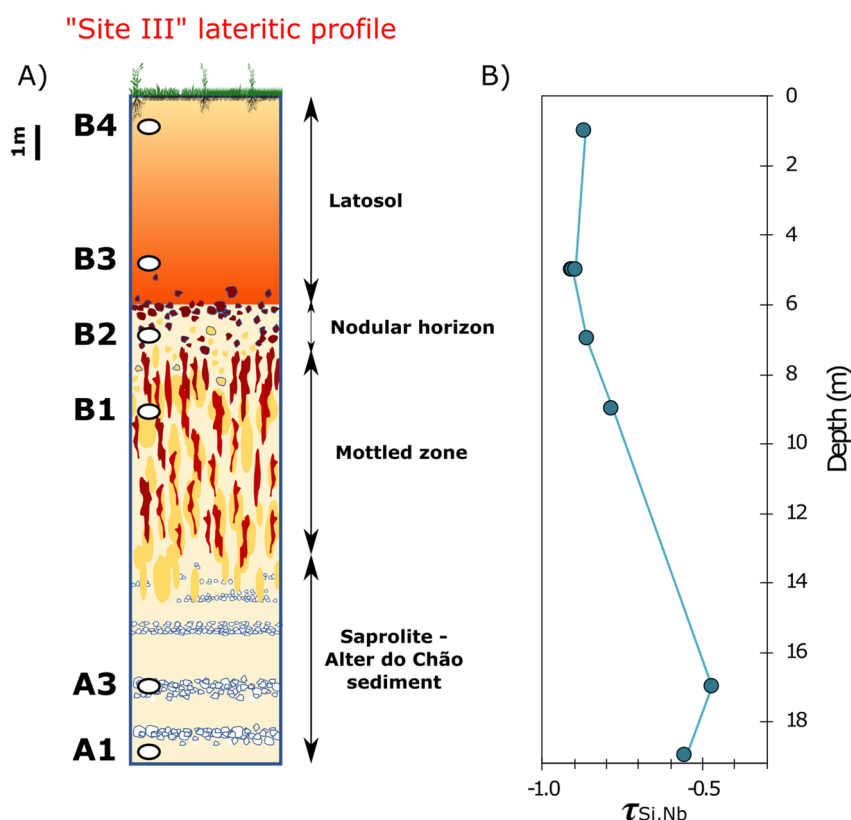


Figure 1. (a) Sketch of the “site III” weathering profile (adapted from Lucas et al., 1996 and Balan et al., 2005). (b) Silicon mass transfer coefficients ($\tau_{Si,Nb}$, using Upper Continental Crust, UCC, as a reference) in the lateritic “site III” weathering profile.

deferrated following the protocol of Mehra and Jackson (1960). These fractions are typically kaolinite and gibbsite-rich, especially in samples B1 to B4. Since silicates are insensitive to the protocol of iron oxide removal, no effect on Si isotope signatures is expected during this step. Sample A1, collected in the saprolite, was analyzed as bulk, that is, without extraction of clay-sized material, because of its pure kaolinite composition. Isotope signatures are reported using the $\delta^{30}\text{Si}$ notation relative to the NBS28 quartz sand international standard. Detailed analytical techniques can be found in section S1 of the Supplementary file.

3. Results

The chemical composition of the lateritic clay-sized fractions can be found in Table S3. Chemical transfers throughout the weathering profile are quantified using mass transfer coefficients ($\tau_{X,Nb}$ in Figure S2 and Table S4) using Nb as an immobile element during chemical weathering. The composition of the upper continental crust (UCC; Rudnick & Gao, 2014) was used as a reference source rock. This is valid given that the Alter do Chão Formation, from which the studied lateritic profile developed, is a detritic rock thought to derive from granitic and granodioritic rocks from the Guyana-Brazilian shields. Throughout the laterite profile, soluble elements such as Na, Ca, Mg, or K are totally depleted ($\tau_{X,Nb} < -0.95$) whereas the $\tau_{X,Nb}$ values of immobile elements (e.g., Ti, Zr, Th) are constant, meaning that these elements behave as Nb (Figure S2a). Alter do Chão sediments are enriched in light rare earth elements (REEs) and undergo continuous leaching from bottom to top (Figures S2c–S2d). Across the profile, the abundance of Si is similar to those of Ga, Al, and V (Figure S2b), with only moderate depletion in the Alter do Chão parent material ($\tau_{Si,Nb} = -0.5$), but intense desilication ($\tau_{Si,Nb} = -0.9$) in the latosol (Figure 1b).

The Alter do Chão kaolinite Si isotope composition ($-0.60 \pm 0.05\text{‰}$) is lighter to the UCC value ($\delta^{30}\text{Si} = -0.25 \pm 0.16\text{‰}$; Savage et al., 2013), but an ever stronger enrichment in light isotopes (by up to $-2.86 \pm 0.05\text{‰}$) is observed from the bottom (14 m) to the top of the lateritic profile (Figure 2a).

4. Discussion

4.1. Timing of Deposition and Weathering of the Alter do Chão Formation

The Alter do Chão Formation consists of stratified sandy clay deposits with sand intercalations. At our particular sampling site, the preservation of deposition structures in the Alter do Chão layer at the bottom of the lateritic profile implies that this horizon can be considered as a saprolite that has experienced nearly isovolumetric weathering. The depletion of Si ($\tau_{\text{Si,Nb}}$ of -0.5 , Figure 1b) and the light Si isotope enrichment ($\delta^{30}\text{Si} = -0.60 \pm 0.05\text{‰}$, Figure 2a) of the Alter do Chão Formation compared with the UCC composition are also consistent with a weathering episode forming secondary kaolinite at the expense of quartz and other Si-bearing primary minerals, as previously observed in other weathering profiles (Opfergelt et al., 2012). However, the $\delta^{30}\text{Si}$ values of kaolinites from the Alter do Chão Formation are about 1.0–1.5‰ heavier than $\delta^{30}\text{Si}$ values for kaolinites formed under similar humid and warm tropical climates (Opfergelt et al., 2010, 2012; Ziegler et al., 2005), and up to 2.2‰ heavier than the $\delta^{30}\text{Si}$ values of kaolinites from the latosol overlying the saprolite part of the profile (Figure 2a).

Variation in the Si isotope composition of kaolinite might stem from the Si isotope composition of the solution from which the kaolinite forms, and/or from the Si isotope fractionation factor prevailing during the formation of the kaolinite. Experimental silica precipitation from an Al-rich solution (Oelze et al., 2015) can be useful in assessing the latter effect. Oelze et al. (2014, 2015) suggest that Si isotope fractionation during silicate precipitation is likely linked with a preliminary step of polysilicic acid adsorption onto Al-hydroxides, leading to the formation of hydroxylaluminosilicates. Due to the longer characteristic time for Si isotope re-equilibration (ca. 2 months) compared to transition elements (a few hours), a strong kinetic isotope fractionation ($\Delta^{30}\text{Si}_{\text{kaolinite-H4SiO4-kin}} = 1000\ln \alpha_{\text{kin}}$ up to -5‰) can be recorded during kaolinite formation at high precipitation rates. A shift from kinetically driven to equilibrium-driven ($\Delta^{30}\text{Si}_{\text{kaolinite-H4SiO4-eq}} = 1000\ln \alpha_{\text{eq}}$) isotope fractionation is observed when precipitation rates slow down (Oelze et al., 2015). Results from experimental (Fernandez et al., 2019; Oelze et al., 2015) and theoretical (Dupuis et al., 2015) studies converge to establish an α_{eq} value of 1 for the processes relevant to weathering in supergene formation. The close-to-UCC $\delta^{30}\text{Si}$ values of the kaolinites present in the Alter do Chão sediments are thus consistent with (a) primary minerals contained in the Alter do Chão sediment serving as the source of Si to these kaolinites and (b) slow formation of kaolinite thereby allowing at least partial isotope equilibration and a low apparent fractionation.

In order to link these isotopic signatures to the environmental conditions prevailing during the corresponding weathering episode, the isotope-enabled reactive transport software CrunchTope was used (details in Text S2). CrunchTope couples a reactive transport model component that numerically solves the mass conservation equation during transport and mineral-fluid interactions, with an isotope component that incorporates isotope-specific rate laws to describe isotope partitioning during mineral-solution reactions (e.g., precipitation of secondary minerals) due to the respective contributions of kinetic and equilibrium isotope fractionation (Steeffel et al., 2015). Originally developed by De Paolo (2011) for steady-state conditions, this framework is based on the transition state theory which allows the model to account for isotope equilibration between the solid phase and the solution through time (Druhan et al., 2013). Initial model conditions such as parent material, soil solution, or rainfall compositions were constrained using geological and geochemical observations reported for the study area (details in Text S2). We estimated that the initial domain consists of a 40-m thick layer of the Alter do Chão sediment composed of K-feldspar, quartz, and muscovite (Horbe et al., 2006) with a porosity of 0.35 (Kamann et al., 2007). As in our model weathering is the result of a balance between infiltration rate and reactivity, this domain was subjected to downward water infiltration and upward supply of fresh bedrock at various rates (Table S1) for simulation times up to 30 Myrs. The model results were then compared with the observed mineralogical (75% kaolinite and 25% quartz), geochemical ($\tau_{\text{Si,Nb}} \sim -0.5$), and isotopic ($\delta^{30}\text{Si} \sim -0.6\text{‰}$) compositions of the Alter do Chão layer currently present at the base of the studied lateritic profile (Figure S9). Model outputs accurately reproduced these values after ~ 15 Myr of simulation time using an infiltration rate of 0.7 m/yr, and a saprolite

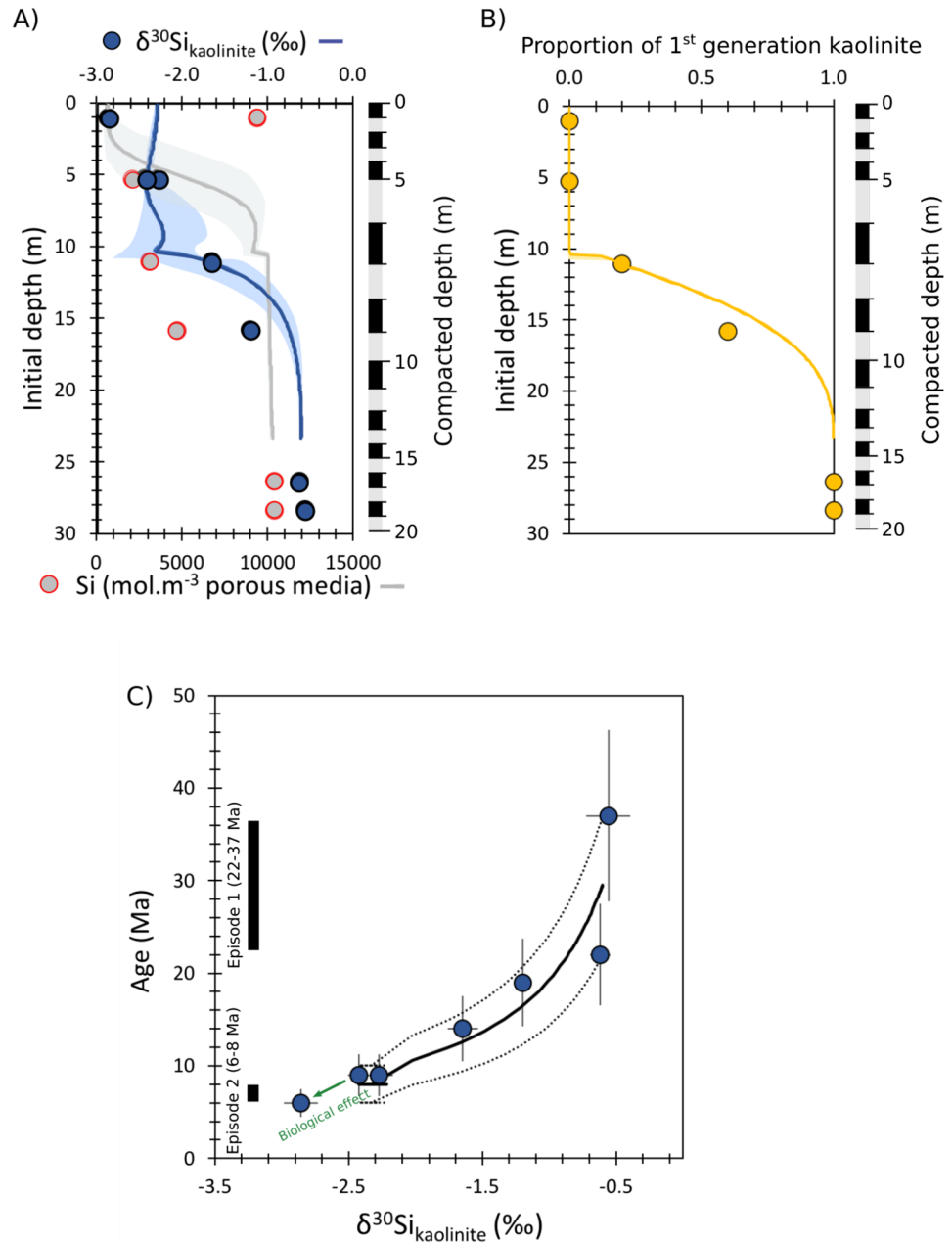


Figure 2. Observed (circles) and modeled (solid line, using reactive transport simulations) (a) kaolinite $\delta^{30}\text{Si}$ values (upper X-axis) and Si content (lower X-axis) versus initial depth (before compaction). (b) Fraction of first-generation kaolinite versus initial depth. (c) Relationship between kaolinite $\delta^{30}\text{Si}$ values and EPR age. In panels (a) and (b), the columns on the right represent the magnitude of vertical decompaction calculated based on Nb concentration, required to compare modeling results with the data (Text S2). In panels (a) and (b), modeled $\delta^{30}\text{Si}$ values, Si content and kaolinite age associated with a variation of $\pm 10\%$ of the infiltration rate value (3.6–4.4 m/yr) during weathering episode 2 are reported as blue, gray, and yellow shaded areas, respectively. In panel C, the three curves differ by the ages of the two weathering episodes (8–6 and 37–22 Ma), with dotted lines reflecting youngest and oldest estimates of their age, and the solid line the central estimate.

production rate of 4 m/Myr. The inferred infiltration rate is half that of the modern maximum infiltration observed in the Rio Negro basin (Maeda et al., 2017), while the saprolite production rate is in the lower range of saprolite production and denudation rates reported in lateritic contexts (Dequincey et al., 2002; Gaillardet et al., 1997; Mathieu et al., 1995; Wittmann, von Blanckenburg, Maurice, Guyot, & Kubik, 2011). Therefore, data and model results are consistent and point to post-depositional alteration of the Alter do Chão sediments by a long, but moderately intense weathering episode. This inference is also consistent with the low-defect structure of Alter do Chão kaolinites (Balan et al., 2005).

A lateritic nature for the Alter do Chão sediment source (e.g., Putzer, 1984) cannot be totally ruled out. However, the presence of kaolinitized feldspars (Irion, 1984) together with our own Si isotope analysis of the Alter do Chão sediment suggest that the conditions prevailing during weathering of this sediment source before its deposition were drastically different from the ones that have led to lateritization, as recorded in the upper horizons of our weathering profile.

Sedimentary kaolinites of ~35–20 Ma age were recorded in different Alter do Chão outcrops in the region of Manaus (Balan et al., 2005). An Oligocene (34–23 Ma) weathering episode is thus likely. The relatively low infiltration rates inferred in our model should thus coincide with the cooler and drier climate at low latitudes thought to characterize the Oligocene (Tardy & Roquin, 2000; Vasconcelos, 1999). The development of an iron crust at the boundary between the Alter do Chão and Novo Remanso sedimentary formations in the Southern part of the Amazon Basin, dated at 45–18 Ma (Gautheron et al., 2020) would imply that this weathering episode could have spread over the whole Amazon Basin, with a northward decline in intensity.

4.2. Record of a Late Miocene Weathering Episode

Observations across the whole profile show that lateritization of the Alter do Chão sediment caused a gradual desilication and enrichment of light Si isotopes in kaolinite (by up to -2.2‰ ; Figure 2) from bottom to top. The kaolinite age gradient throughout the profile suggests that kaolinite formation and Si isotope signatures can be explained by two scenarios: (a) a slow and continuous kaolinite replacement occurring throughout the period between 37–22 and 8–6 Ma or (b), as suggested by Balan et al. (2005), a two-component mixing (curved line in Figure 2c) between kaolinites inherited from the post-depositional weathering episode of the Alter do Chão formation (37–22 Ma), and "new" kaolinites replacing the first population during a single discrete, later weathering episode at 8–6 Ma. Several observations argue in favor of the latter scenario. A similar age profile with depth was recorded in three distinct lateritic profiles overlying Alter do Chão sediments (Figure S3, Balan et al., 2005), with a 8–6 Ma age determined for kaolinite in their top 5 m latosols (Figure S4). These observations are consistent with kaolinite replacement occurring 8–6 Ma ago, from the top to the bottom of the profile at a similar rate over the whole Alter do Chão formation. Additionally, as precipitation rates slow down, Si isotopes are increasingly able to equilibrate between the fluid and solid phases. Thus the observed depletion of light Si isotopes in the upper horizons of the laterite is incompatible with slow and continuous kaolinite replacement over several tens of Myrs. Finally, the existence of the "Late Velhas" lateritization episode, dated at 10 Ma using paleomagnetism in French Guyana (Théveniaut & Freyssinet, 2002), supports the occurrence of a short-term weathering episode spread over the whole Amazon Basin in the Miocene.

The relationship we observe between kaolinite age and the $\delta^{30}\text{Si}$ over the profile (Figure 2c) supports a two-end-member mixing scenario with increasing proportion of "new" kaolinite toward the surface at the expense of kaolinite formed during the first post-depositional episode of weathering of the Alter do Chão formation described above. As explained in Section 4.1, the strong enrichment of new kaolinite in light Si isotopes requires fast formation to preserve a record of kinetic isotope fractionation. Such a fast rate of formation is further supported by the low degree of crystallinity observed in this second generation of kaolinites (Balan et al., 2005). In addition, it is apparent that this episode of replacement must have ceased prior to completion in order for both kaolinite population to still coexist. As performed above for the first weathering episode, isotope-enabled reactive transport simulations (details in Text S2) were used to determine the most likely timing and conditions supporting this second weathering episode. Initial conditions were set as for the first weathering episode, with the notable exceptions of porosity (0.5) and initial mineralogy (95% kaolinite – 5% quartz) updated to reflect the characteristics of a previously weathered Alter do Chão formation (Figures S6 and S7). To account for the non-isovolumetric weathering of this episode, artificial

“decompaction” of the modern weathering profile was performed based on the Nb concentrations, a weathering-resistant element (Figure S10). Results show that Si isotope signature of kaolinite (Figure 2a), observed kaolinite replacement (Figure 2b), and $\delta^{30}\text{Si}$ -age relationship (Figure 2c) can be correctly reproduced after a 2-Myr long episode with relatively fast water infiltration (4 m/yr) and moderate saprolite production (7.5 m/Myr). The micro-aggregated structure of the latosol (pseudo-sands of latosols, Fritsch et al., 2002) is consistent with an enhanced water infiltration rate in comparison with the first weathering episode. The structuration of the latosol is thus a critical factor for the evolution of the profile. Thus, the model results indicate that enhanced water infiltration through the profile is likely responsible for the observed kaolinite replacement during this second weathering episode.

The inferred timing (6–8 Ma) and intensity of this second weathering episode are consistent with the warm, humid, and seasonally contrasted climate thought to prevail over the Amazon during late Miocene. Indeed, this period sees the onset of the transcontinental Amazon River, that may have modified climatic conditions, vegetation cover or seasonality in the basin and thus the water drainage across the basin (Figueiredo et al., 2009). Because the youngest kaolinites in the latosol have a 6 Ma age, it is likely that such extreme climatic conditions have not been encountered since.

However, significant discrepancies remain between the modeled and measured Si content in the lateritic profile (Figure 2a). The model results suggest that kaolinite replacement during the second episode occurred without substantial Si loss. The Si loss observed in the top of the profile thus suggests that desilication may have taken place after this episode, synchronously with the transformation of iron oxides (hematite/goethite to aluminous goethite) and the precipitation of gibbsite (Balan et al., 2007; Fritsch et al., 2002, 2005). Second, while the model predicts kaolinite dissolution and gibbsite precipitation in the top 5 m of the profile (Figure S13), a kaolinite-rich latosol layer is actually present there. This discrepancy can be attributed to the existence of other processes promoting kaolinite stabilization not accounted for in our model, for example biological cycling. Lucas et al. (1993) proposed that Si overturning by aboveground vegetation can cause Si enrichment in percolating fluids, thereby limiting kaolinite destabilization in the upper soil horizons.

4.3. The Effect of the Silicon Biological Cycle on Topsoil

We contend that the impact of biological cycling on Si is restricted to the topmost part of the lateritic profile. Such impact may be direct or indirect. Fast, microbiologically mediated weathering of kaolinite was reported in the topmost 40 cm of a lateritic profile following mineral aging experiments (Cornu et al., 1995). An indirect action is also plausible through the stabilization of kaolinite in topsoil due to biologically driven changes in soil solution chemistry (Lucas et al., 1993). Recent, biologically induced kaolinite formation could explain the youngest kaolinite age (6 Ma) recorded for the latosol sample of our profile compared with deeper samples and with latosols sampled elsewhere and dated at 8 Ma. Partial kaolinite recrystallization is also supported by a one-third decrease in radiation-induced defects observed in our topmost sample (Balan et al., 2005). The $\tau_{\text{Si,Nb}}$ slight increase (while Nb concentrations remain constant) in this layer compared to layers below is also consistent with a biological control on Si since Nb is mostly located in refractory minerals and not involved in biological overturning. Therefore, the kaolinite age in the topmost layer (sample B4) is most likely the result of mixing between a dominant population of disordered kaolinite formed at 8 Ma (second weathering episode above) and a minor pool of more recent kaolinite, the formation of which was aided by biological cycling. This interpretation is in agreement with the lighter $\delta^{30}\text{Si}$ values measured in latosol samples as biological uptake favors light isotopes (see review by Sutton et al., 2018) and thus has the ability to promote a topsoil Si pool depleted in heavy isotopes and available for kaolinite precipitation.

5. Conclusions

In this study, we demonstrate for the first time that Si isotopes recorded in laterite-forming minerals can be used in combination with dating tools to effectively reconstruct past continental weathering conditions. We applied this approach to a well-studied lateritic weathering profile in the Amazon Basin, near Manaus, Brazil. The evolution of this laterite profile is sketched in Figure 3 and is consistent with the episodic nature of weathering phases leading to the formation of laterites (Vasconcelos et al., 1994). After sediment deposition, our geochemical results supported by an isotope-enabled reactive transport model show that the

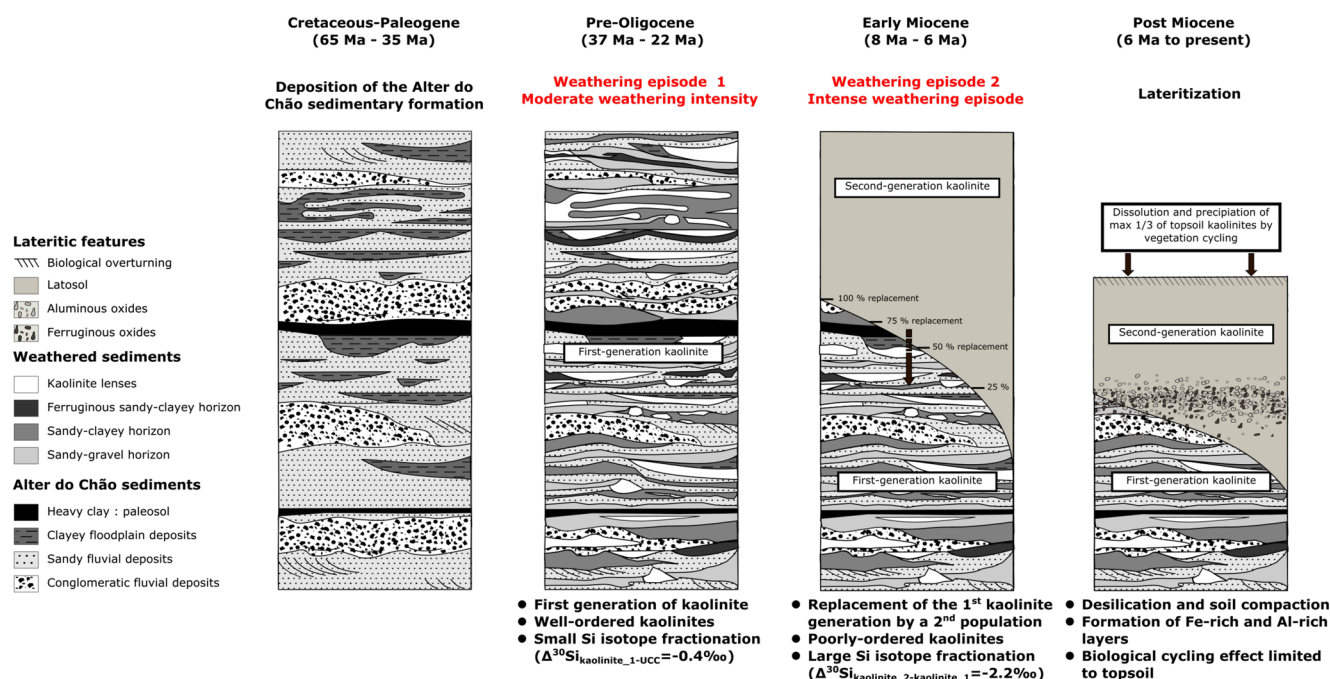


Figure 3. Sketch for the evolution of the studied lateritic profile from the deposition of the Alter do Chão sedimentary formation (35–65 Ma) to present day. Sequence of the weathered Alter do Chão sediments and of the developed lateritic profile are inspired by Montes et al. (2002) and Lucas (1989), respectively.

study area underwent, at least, two major weathering episodes, which were distinct in their intensity; a first episode (ca. 35–20 Ma) of moderate intensity producing well-crystallized kaolinites from the parent sediment, and a more recent (8–6 Ma) and shorter phase causing the progressive downward replacement of the first kaolinite generation by a new population under conditions of rapid water percolation. Our inference on these two weathering episodes is supported by previously reported paleoclimatic and paleogeographic evidence recorded over the Amazon Basin.

These conclusions show that climatic factors - and in particular rainfall intensity through water infiltration rates—control the timing of chemical weathering processes that generate deeply stratified tropical weathering profiles. This study will have significant bearing on the combined use of Si isotopes, dating techniques, and isotope-enabled reactive transport models to determine past weathering conditions recorded in tropical profiles, and paves the way for future studies aiming at using metal stable isotopes in old weathering profiles as tracers of paleo-environmental conditions on the continents.

Data Availability Statement

All data reported in this study can be found in the supplementary file and are available on the server Zenodo (<https://zenodo.org/record/5514356#.YUURYC0ivfZ>; <https://doi.org/10.5281/zenodo.5514356>) to match the FAIR requirements.

References

- Albert, J. S., Val, P., & Hoorn, C. (2018). The changing course of the Amazon River in the Neogene: Enter stage for Neotropical diversification. *Neotropical Ichthyology*, 16. <https://doi.org/10.1590/1982-0224-20180033>
- Allard, T., Gautheron, C., Bressan Riffel, S., Balan, E., Soares, B. F., Pinna-Jamme, R., et al. (2018). Combined dating of goethites and kaolinites from ferruginous. Deciphering the Late Neogene erosion history of Central Amazonia. *Chemical Geology*, 479, 136–150. <https://doi.org/10.1016/j.chemgeo.2018.01.004>
- Ambrosi, J. P., & Nahon, D. (1986). Petrological and geochemical differentiation of lateritic iron crust profiles. *Chemical Geology*, 57(3), 371–393. [https://doi.org/10.1016/0009-2541\(86\)90059-8](https://doi.org/10.1016/0009-2541(86)90059-8)
- Balan, E., Allard, T., Fritsch, E., Sélo, M., Falguères, C., Chabaux, F., et al. (2005). Formation and evolution of lateritic profiles in the middle Amazon basin: Insights from radiation-induced defects in kaolinite. *Geochimica et Cosmochimica Acta*, 69(9), 2193–2204. <https://doi.org/10.1016/j.gca.2004.10.028>

Acknowledgments

The authors want to thank Pascale Louvat and Nicole Fernandez for assistance on MC-ICP-MS measurements and Pierre Burckel for technical support on Quadrupole ICP-MS analysis. D.G. is financially supported by the ANR RECA (ANR-17-CE01-0012). This work was supported by IPGP multidisciplinary program PARI, and by Paris–IdF region SESAME Grant no. 12015908.

- Balan, E., Allard, T., Morin, G., Fritsch, E., & Calas, G. (2020). *Electron Paramagnetic Resonance Spectroscopy: Applications of clay minerals, weathering processes and evolution of continental surfaces* (pp. 109–135). Cham: Springer International Publishing.
- Balan, E., Fritsch, E., Allard, T., & Calas, G. (2007). Inheritance vs. neoformation of kaolinite during lateritic soil formation. *Clays and Clay Minerals*, 55(3), 253–259. <https://doi.org/10.1346/ccmn.2007.0550303>
- Beauvais, A. (1999). Geochemical balance of processes and climatic signatures in weathering profiles overlain by in Central Africa. *Geochimica et Cosmochimica Acta*, 63(23), 3939–3957. [https://doi.org/10.1016/S0016-7037\(99\)00173-8](https://doi.org/10.1016/S0016-7037(99)00173-8)
- Cornu, S., Lucas, Y., Desjardins, T., & Nitsche, S. (1995). Rapidité de la vitesse d'altération des minéraux du sol en conditions ferrallitiques. Méthode des minéraux-test. *Comptes Rendus de l'Académie des Sciences*, 321, 311–316.
- DePaolo, D. J. (2011). Surface kinetic model for isotopic and trace element fractionation during precipitation of calcite from aqueous solutions. *Geochimica et Cosmochimica Acta*, (4), 1039–1056. <https://doi.org/10.1016/j.gca.2010.11.020>
- Dequincey, O., Chabaux, F., Clauer, N., Sigmarsson, O., Liewig, N., & Leprun, J. C. (2002). Chemical mobilizations in laterites: Evidence from trace elements and 238U-234U-230Th disequilibria. *Geochimica et Cosmochimica Acta*, 66(7), 1197–1210. [https://doi.org/10.1016/S0016-7037\(01\)00845-6](https://doi.org/10.1016/S0016-7037(01)00845-6)
- Druhan, J. L., Steefel, C. I., Williams, K. H., & DePaolo, D. J. (2013). Calcium isotope fractionation in groundwater: Molecular scale processes influencing field scale behavior. *Geochimica et Cosmochimica Acta*, 119, 93–116. <https://doi.org/10.1016/j.gca.2013.05.022>
- Dupuis, R., Benoit, M., Nardin, E., & Méheut, M. (2015). Fractionation of silicon isotopes in liquids: The importance of configurational disorder. *Chemical Geology*, 396, 239–254.
- Fernandez, N. M., Zhang, X., & Druhan, J. L. (2019). Silicon isotopic re-equilibration during amorphous silica precipitation and implications for isotopic signatures in geochemical proxies. *Geochimica et Cosmochimica Acta*, 262, 104–127. <https://doi.org/10.1016/j.gca.2019.07.029>
- Figueiredo, J., Hoorn, C., van der Ven, P., & Soares, E. (2009). Late Miocene onset of the Amazon River and the Amazon deep-sea fan: Evidence from the Foz do Amazonas Basin. *Geology*, 37(7), 619–622. <https://doi.org/10.1130/G25567a.1>
- Fritsch, E., Montes-Lauar, C. R., Boulet, R., Melfi, A. J., Balan, E., & Magat, P. (2002). Lateritic and redoximorphic features in a faulted landscape near Manaus, Brazil. *European Journal of Soil Science*, 53, 203–217. <https://doi.org/10.1046/j.1351-0754.2002.00448.x>
- Fritsch, E., Morin, G., Bedidi, A., Bonnin, D., Balan, E., Caquineau, S., & Calas, G. (2005). Transformation of haematite and Al-poor goethite to Al-rich goethite and associated yellowing in a clay soil profile of the middle Amazon Basin (Manaus, Brazil). *European Journal of Soil Science*, (5), 575–588. <https://doi.org/10.1111/j.1365-2389.2005.00693.x>
- Gaillardet, J., Dupre, B., Allegre, C. J., & Négrel, P. (1997). Chemical and physical denudation in the Amazon River Basin. *Chemical Geology*, 142(3–4), 141–173. [https://doi.org/10.1016/S0009-2541\(97\)00074-0](https://doi.org/10.1016/S0009-2541(97)00074-0)
- Gautheron, C., Cabriolu, C., Pupim, F., Parra, M., Schwartz, S., Pinna-Jamme, R., et al. (2020). Paleogene to Quaternary geodynamical evolution of the lowland Central Amazonia inferred by weathering phases dating: Online (pp. EGU2020–8407).
- Giral-Kacmarcik, S., Savin, S. M., Nahon, D. B., Girard, J.-P., Lucas, Y., & Abel, L. J. (1998). Oxygen isotope geochemistry of kaolinite in laterite-forming processes, Manaus, Amazonas, Brazil. *Geochimica et Cosmochimica Acta*, 62(11), 1865–1879.
- Girard, J.-P., Freyssinet, P., & Chazot, G. (2000). Unraveling climatic changes from intraprofile variation in oxygen and hydrogen isotopic composition of goethite and kaolinite in laterites: Integrated study from Yaou. *Geochimica et Cosmochimica Acta*, 64(3), 409–426. [https://doi.org/10.1016/S0016-7037\(99\)00299-9](https://doi.org/10.1016/S0016-7037(99)00299-9)
- Girard, J.-P., Razanadranoroa, D., & Freyssinet, P. (1997). Laser oxygen isotope analysis of weathering goethite from the lateritic profile of Yaou, French Guiana: Paleoweathering and paleoclimatic implications. *Applied Geochemistry*, 12(2), 163–174. [https://doi.org/10.1016/S0883-2927\(96\)00062-5](https://doi.org/10.1016/S0883-2927(96)00062-5)
- Hoorn, C., Bogotá-A, G. R., Romero-Baez, M., Lammertsma, E. I., Flantua, S. G. A., Dantas, E. L., et al. (2017). The Amazon at sea: Onset and stages of the Amazon River from a marine record, with special reference to Neogene plant turnover in the drainage basin. *Global and Planetary Change*, 153, 51–65. <https://doi.org/10.1016/j.gloplacha.2017.02.005>
- Hoorn, C., Roddaz, M., Dino, R., Soares, E., Uba, C., Ochoa-Lozano, D., & Mapes, R. (2010a). The Amazonian Craton and its influence on past fluvial systems (Mesozoic-Cenozoic, Amazonia): *Amazonia: Landscape and Species Evolution: A Look Into the Past*, 103–122.
- Hoorn, C., Wesselingh, F. P., ter Steege, H., Bermudez, M. A., Mora, A., Sevink, J., et al. (2010b). Amazonia through time: Andean uplift, climate change, landscape evolution, and biodiversity. *Science*, 330(6006), 927–931. <https://doi.org/10.1126/science.1194585>
- Horbe, A. M. C., Vieira, L. C., & Nogueira, A. C. R. (2006). Geoquímica de camadas vermelhas bioturbadas da Formação Alter do Chão. *Revista Brasileira de Geociências*, 36(3), 396–402. <https://doi.org/10.25249/0375-7536.2006363396402>
- Irion, G. (1984). Clay minerals of Amazonian soils. In H. J. Dumont (Ed.), *The Amazon* (pp. 537–569). https://doi.org/10.1007/978-94-009-6542-3_21
- Kamann, P. J., Ritzi, R. W., Dominic, D. F., & Conrad, C. M. (2007). Porosity and permeability in sediment mixtures. *Groundwater*, 45(4), 429–438. <https://doi.org/10.1111/j.1745-6584.2007.00313.x>
- Lucas, Y. (1989). *Systèmes pédologiques en Amazonie brésilienne*. (p. 157).
- Lucas, Y., Luizao, F. J., Chauvel, A., Rouiller, J., & Nahon, D. (1993). The relation between biological activity of the rain forest and mineral composition of soils. *Science*, 260(5107), 521–523. <https://doi.org/10.1126/science.260.5107.521>
- Lucas, Y., Nahon, D., Cornu, S., & Eyrolle, F. (1996). Genèse et fonctionnement des sols en milieu équatorial. *Sciences de la Terre*, 322(1), 1–16.
- Maeda, E. E., Ma, X., Wagner, F. H., Kim, H., Oki, T., Eamus, D., & Huete, A. (2017). Evapotranspiration seasonality across the Amazon Basin. *Earth System Dynamics*, 8(2), 439–454. <https://doi.org/10.5194/esd-8-439-2017>
- Maher, K., Steefel, C. I., White, A. F., & Stonestrom, D. A. (2009). The role of reaction affinity and secondary minerals in regulating chemical weathering rates at the Santa Cruz Soil Chronosequence, California. *Geochimica et Cosmochimica Acta*, 73(10), 2804–2831. <https://doi.org/10.1016/j.gca.2009.01.030>
- Mathian, M., Bueno, G. T., Balan, E., Fritsch, E., Do Nascimento, N. R., Selo, M., & Allard, T. (2020). Kaolinite dating from and: A new key to understanding the landscape evolution in NW Amazonia (Brazil). *Geoderma*, 370, 114354. <https://doi.org/10.1016/j.geoderma.2020.114354>
- Mathieu, D., Bernat, M., & Nahon, D. (1995). Short-lived U and Th isotope distribution in a tropical laterite derived from granite (river basin, Amazonia, Brazil): Application to assessment of weathering rate. *Earth and Planetary Science Letters*, 136(3), 703–714. [https://doi.org/10.1016/0012-821X\(95\)00199-m](https://doi.org/10.1016/0012-821X(95)00199-m)
- Mehra, O. P., & Jackson, M. L. (1960). Iron oxide removal from soils and clays by a dithionite-citrate system buffered with sodium bicarbonate. In E. Ingerson (Ed.), *Clays and Clay Minerals* (pp. 317–327). Pergamon.
- Mendes, A. C., Truckenbrod, W., & Nogueira, A. C. R. (2012). Análise faciológica da Formação Alter do Chão (Cretáceo, Bacia do Amazonas), próximo à cidade de Óbidos, Pará. *Revista Brasileira de Geociências*, 42(1), 39–57. <https://doi.org/10.25249/0375-7536.20124213957>

- Monteiro, H. S., Vasconcelos, P. M. P., Farley, K. A., & Lopes, C. A. M. (2018). Age and evolution of diachronous erosion surfaces in the Amazon: Combining (U-Th)/He and cosmogenic ^3He records. *Geochimica et Cosmochimica Acta*, 229, 162–183. <https://doi.org/10.1016/j.gca.2018.02.045>
- Montes, C. R., Melfi, A. J., Carvalho, A., Vieira-Coelho, A. C., & Formoso, M. L. (2002). Genesis, mineralogy and geochemistry of kaolin deposits of the Jari River. *Clays and Clay Minerals*, 50(4), 494–503. <https://doi.org/10.1346/000986002320514217>
- Muller, J.-P., & Calas, G. (1989). Tracing kaolinites through their defect centers; kaolinite paragenesis in a laterite (Cameroon). *Economic Geology*, 84(3), 694–707. <https://doi.org/10.2113/gsecongeo.84.3.694>
- Nahon, D. (2003). Altérations dans la zone tropicale. Signification à les mécanismes anciens et/ou encore. *Comptes Rendus Geoscience*, 335(16), 1109–1119. <https://doi.org/10.1016/j.crte.2003.10.008>
- Oelze, M., von Blanckenburg, F., Bouchez, J., Hoellen, D., & Dietzel, M. (2015). The effect of Al on Si isotope fractionation investigated by silica precipitation experiments. *Chemical Geology*, 397, 94–105. <https://doi.org/10.1016/j.chemgeo.2015.01.002>
- Oelze, M., von Blanckenburg, F., Hoellen, D., Dietzel, M., & Bouchez, J. (2014). Si stable isotope fractionation during adsorption and the competition between kinetic and equilibrium isotope fractionation: Implications for weathering systems. *Chemical Geology*, 380, 161–171. <https://doi.org/10.1016/j.chemgeo.2014.04.027>
- Opfergelt, S., Cardinal, D., André, L., Delvigne, C., Bremond, L., & Delvaux, B. (2010). Variations of $\delta^{30}\text{Si}$ and Ge/Si with weathering and biogenic input in tropical basaltic ash soils under monoculture. *Geochimica et Cosmochimica Acta*, 74(1), 225–240. <https://doi.org/10.1016/j.gca.2009.09.025>
- Opfergelt, S., Georg, R. B., Delvaux, B., Cabidoche, Y. M., Burton, K. W., & Halliday, A. N. (2012). Silicon isotopes and the tracing of desilication in volcanic soil weathering sequences. *Chemical Geology*, 326–327, 113–122. <https://doi.org/10.1016/j.chemgeo.2012.07.032>
- Putzer, H. (1984). The geological evolution of the Amazon basin and its mineral resources. In H. Sioli (Ed.), *The Amazon: Limnology and landscape ecology of a mighty tropical river and its basin* (pp. 15–46). Springer Netherlands. https://doi.org/10.1007/978-94-009-6542-3_2
- Retallack, G. J. (2010). Lateritization and bauxitization events. *Economic Geology*, 105(3), 655–667. <https://doi.org/10.2113/gsecongeo.105.3.655>
- Rudnick, R. L., & Gao, S. (2014). 4.1-Composition of the continental crust A2. In H. D. Holland, & K. K. Turekian (Eds.), *Treatise on geochemistry* (pp. 1–51). Elsevier. <https://doi.org/10.1016/b978-0-08-095975-7.00301-6>
- Ruffet, G., Innocent, C., Michard, A., Féraud, G., Beauvais, A., Nahon, D., & Hamelin, A. N. (1996). A geochronological $^{40}\text{Ar}/^{39}\text{Ar}$ and $^{87}\text{Rb}/^{81}\text{Sr}$ study of K-Mn oxides from the weathering sequence of Azul, Brazil. *Geochimica et Cosmochimica Acta*, 60(12), 2219–2232. [https://doi.org/10.1016/0016-7037\(96\)00080-4](https://doi.org/10.1016/0016-7037(96)00080-4)
- Savage, P. S., Georg, R. B., Williams, H. M., & Halliday, A. N. (2013). The silicon isotope composition of the upper continental crust. *Geochimica et Cosmochimica Acta*, 109, 384–399. <https://doi.org/10.1016/j.gca.2013.02.004>
- Steeffel, C. I., Appelo, C. A. J., Arora, B., Jacques, D., Kalbacher, T., Kolditz, O., et al. (2015). Reactive transport codes for subsurface environmental simulation. *Computational Geosciences*(3), 445–478. <https://doi.org/10.1007/s10596-014-9443-x>
- Sutton, J. N., André, L., Cardinal, D., Conley, D. J., de Souza, G. F., Dean, J., et al. (2018). A Review of the stable isotope bio-geochemistry of the global silicon cycle and its associated trace elements. *Frontiers Earth Science*, 5(112). <https://doi.org/10.3389/feart.2017.00112>
- Tardy, Y., & Roquin, C. (2000). Dérive des continents: Paléoclimats et distribution des couvertures pédologiques tropicales (Continental drift: Paleoclimates and distribution of the pedological tropical covers). *Bulletin de l'Association de Géographes Français*, 373–383. <https://doi.org/10.3406/bagf.2000.2185>
- Théveniaut, H., & Freyssinet, P. (2002). Timing of on the Guiana Shield: Synthesis of paleomagnetic results from French Guiana and Suriname. *Palaeogeography, Palaeoclimatology, Palaeoecology*, 178(1), 91–117. [https://doi.org/10.1016/s0031-0182\(01\)00404-7](https://doi.org/10.1016/s0031-0182(01)00404-7)
- Vasconcelos, P. M. (1999). K-Ar and $^{40}\text{Ar}/^{39}\text{Ar}$ geochronology of weathering processes. *Annual Review of Earth and Planetary Sciences*(1), 183–229. <https://doi.org/10.1146/annurev.earth.27.1.183>
- Vasconcelos, P. M., Renne, P. R., Brimhall, G. H., & Becker, T. A. (1994). Direct dating of weathering phenomena by $^{40}\text{Ar}/^{39}\text{Ar}$ and K-Ar analysis of supergene K-Mn oxides. *Geochimica et Cosmochimica Acta*, 58(6), 1635–1665. [https://doi.org/10.1016/0016-7037\(94\)90565-7](https://doi.org/10.1016/0016-7037(94)90565-7)
- Wittmann, H., von Blanckenburg, F., Maurice, L., Guyot, J. L., & Kubik, P. W. (2011b). Recycling of Amazon floodplain sediment quantified by cosmogenic ^{26}Al and ^{10}Be . *Geology*, 39(5), 467–470. <https://doi.org/10.1130/g31829.1>
- Ziegler, K., Chadwick, O. A., White, A. F., & Brzezinski, M. A. (2005). $\delta^{30}\text{Si}$ systematics in a granitic saprolite, Puerto Rico. *Geology*, 33(10), 817–820. <https://doi.org/10.1130/g21707.1>

References From the Supporting Information

- Benedetti, M. F., Mounier, S., Filizola, N., Benaim, J., & Seyler, P. (2003). Carbon and metal concentrations, size distributions and fluxes in major rivers of the Amazon basin. *Hydrological Processes*, 17(7), 1363–1377.
- Cornu, S., Lucas, Y., Ambrosi, J. P., & Desjardins, T. (1998). Transfer of dissolved Al, Fe and Si in two Amazonian forest environments in Brazil. *European Journal of Soil Science*, 49(3), 377–384.
- Dosseto, A., Turner, S. P., & Chappell, J. (2008). The evolution of weathering profiles through time: New insights from uranium-series isotopes. *Earth and Planetary Science Letters*, 274(3), 359–371.
- Dupuis, R., Benoit, M., Nardin, E., & Méheut, M. (2015). Fractionation of silicon isotopes in liquids: The importance of configurational disorder. *Chemical Geology*, 396, 239–254.
- Eyrolle, F., Benedetti, M. F., Benaim, J. Y., & Février, D. (1996). The distributions of colloidal and dissolved organic carbon, major elements, and trace elements in small tropical catchments. *Geochimica et Cosmochimica Acta*, 60(19), 3643–3656.
- Frings, P. J., Clymans, W., Fontorbe, G., De La Rocha, C. L., & Conley, D. J. (2016). The continental Si cycle and its impact on the ocean Si isotope budget. *Chemical Geology*, 425, 12–36.
- Geilert, S., Vroon, P. Z., Keller, N. S., Gudbrandsson, S., Stefánsson, A., & van Bergen, M. J. (2015). Silicon isotope fractionation during silica precipitation from hot-spring waters: Evidence from the geothermal field, Iceland. *Geochimica et Cosmochimica Acta*, 164, 403–427.
- Honório, B. A. D., Horbe, A. M. C., & Seyler, P. (2010). Chemical composition of rainwater in western Amazonia — Brazil. *Atmospheric Research*, 98(2), 416–425.
- Jochum, K. P., Weis, U., Schwager, B., Stoll, B., Wilson, S. A., Haug, G. H., et al. (2016). Reference values following ISO guidelines for frequently requested rock reference materials. *Geostandards and Geoanalytical Research*, 40(3), 333–350.
- Méheut, M., & Schauble, E. A. (2014). Silicon isotope fractionation in silicate minerals: Insights from first-principles models of phyllosilicates, albite and pyrope. *Geochimica et Cosmochimica Acta*, 134, 137–154.

- Palandri, J. L., & Kharaka, Y. K. (2004). A compilation of rate parameters of water-mineral interaction kinetics for application to geochemical modeling: Geological Survey Menlo Park CA.
- Poitrasson, F. (2017). Silicon isotope geochemistry. *Reviews in Mineralogy and Geochemistry*, 82(1), 289–344.
- Poszwa, A., Dambrine, E., Ferry, B., Pollier, B., & Loubet, M. (2002). Do deep tree roots provide nutrients to the tropical rainforest? *Biogeochemistry*(1), 97–118.
- Roerdink, D. L., van den Boorn, S. H. J. M., Geilert, S., Vroon, P. Z., & van Bergen, M. J. (2015). Experimental constraints on kinetic and equilibrium silicon isotope fractionation during the formation of non-biogenic chert deposits. *Chemical Geology*, 402, 40–51.
- Sawe, B. (2019). *Wettest places on Earth by annual rainfall*. Retrieved from <https://www.worldatlas.com/articles/the-ten-wettest-places-in-the-world.html>
- Sioli, H. (1984). The Amazon and its main affluents: Hydrography, morphology of the river courses, and river types. In H. J. Dumont (Ed.), *The Amazon* (pp. 121–165).
- Steefel, C. I., Druhan, J. L., & Maher, K. (2014). Modeling coupled chemical and isotopic equilibration rates: *Procedia Earth and Planetary Science*, 10, 208–217.
- Steinhofel, G., Breuer, J., von Blanckenburg, F., Horn, I., & Sommer, M. (2017). The dynamics of Si cycling during weathering in two small catchments in the Black Forest (Germany) traced by Si isotopes. *Chemical Geology*, 466, 389–402.
- Williams, M. R., Fisher, T. R., & Melack, J. M. (1997). Solute dynamics in soil water and groundwater in a central Amazon catchment undergoing deforestation. *Biogeochemistry*, 38(3), 303–335.
- Wittmann, H., von Blanckenburg, F., Maurice, L., Guyot, J.-L., Filizola, N., & Kubik, P. W. (2011a). Sediment production and delivery in the Amazon River basin quantified by in situ-produced cosmogenic nuclides and recent river loads. *GSA Bulletin*, 123(5–6), 934–950.